

Dynamic load on the head during rear impact against a headrest

Tomasz Pusty^{1*}, Przemysław Simiński², Jerzy Jackowski³,
Ewelina Kostecka⁴, Leszek Chybowski⁵

¹ Department of Machine Construction, Maritime University of Szczecin, ul. Willowa 2, 71-650 Szczecin, Poland

² Department of Development, Military Institute of Armoured and Automotive Technology, ul. Okuniewska 1, 05-070 Sulejów, Poland

³ Department of Mechanical Engineering, Institute of Vehicles and Transportation, Military University of Technology, ul. gen. Sylwestra Kaliskiego 2, 00-908 Warsaw, Poland

⁴ Department of Electrical Engineering and Power Electronics, Faculty of Mechatronics and Electrical Engineering, Maritime University of Szczecin, ul. Willowa 2, 71-650 Szczecin, Poland

⁵ Department of Machine Construction, Maritime University of Szczecin, ul. Willowa 2, 71-650 Szczecin, Poland

* Corresponding author: t.pusty@pm.szczecin.pl

ABSTRACT

A model of the dynamics of a vehicle collision with an energy-absorbing barrier was built in the PC-Crash 10.0 environment, using the following models: vehicle motion dynamics, collision, and multibody models of people seated on seats. The energy-absorbing barrier was composed of connected elements whose motion was described by Newton's and Euler's equations. Rear-seat passengers were modeled as polyhedral systems, each consisting of 20 rigid solids connected by spherical joints. The simulations investigated the effects of different headrest and seatback settings configurations on the dynamic loads acting on the head of a passenger seated in the rear bench seat. The results showed that the value of the coefficient describing the risk of head injury decreased as the backrest tilt angle increased, indicating that the head is better protected with greater tilt. The stiffness of the headrest significantly affected the value of the coefficient describing the risk of head injury, i.e., with a higher stiffness of 20,000 N/m, a strong negative correlation was observed, indicating a lower risk of injury. However, further increases in stiffness may negatively impact the risk of head injuries. In contrast, at lower stiffnesses, the correlation was more variable, with different results depending on the angle of the backrest. The results underscore that proper configuration of the backrest, seat tilt angles, and headrest stiffness are key to minimizing head injuries. Particularly favorable values of the coefficient describing the risk of head injury were achieved at angles of 5° headrest tilt angle and 10° headrest tilt angle and corresponding values of headrest stiffness. In general, a negative correlation was observed between the backrest tilt angle and the HIC_{36ms} value, i.e., the larger the tilt angle, the lower the HIC_{36ms} value, which means better protection. At the lower stiffness of the headrest, 15,000 N/m, the correlation was variable, both positive and negative, depending on the backrest tilt angle.

Keywords: dynamic loads of the head, human dynamics, vehicle collision dynamics.

INTRODUCTION

With the increasing number of traffic accidents and vehicle safety needs, the analysis of rear offset crashes, especially in terms of the dynamic loads acting on the occupants, is becoming a topic of critical importance to modern

automotive engineering. In the context of rapidly changing safety regulations, research into the effectiveness of headrest and seat belts in rear-end crashes is becoming not only timely but also crucial for future design solutions. Over the past five years, changes to The United Nations Economic Commission for Europe (UNECE) Regulation

17 have focused on improving occupant protection, working better with modern technologies, and adapting seats to electric and autonomous vehicles. Requirements for headrest, ISOFIX (International Organization for Standardization – ISO Fixture) systems, dynamic testing, and side impact protection were strengthened. The variety of test dummies has also been increased to reflect real-world conditions and passenger diversity better. The regulation also adapts to changes in the automotive industry, covering new technologies and active safety systems.

With the introduction of modern technologies in vehicles, there is an urgent need to update research on the effectiveness of safety systems to better reflect actual operating conditions. The research presented here is aimed not only at understanding dynamic loads during rear-end crashes but also at providing valuable information for builders and designers, which can ultimately contribute to raising safety standards in the automotive industry. According to recent studies e.g. [1–3], the need to further explore the topic of crashes is obvious, especially in light of the frequent head and neck injuries resulting from crashes, even in low-speed crashes, i.e., up to 25 km/h [4]. Headrests must be placed close to the head, and their height and shape adjusted to protect passengers of different body sizes. Headrests and seats must better absorb impact energy and prevent excessive head and neck deflection. Seats have begun to be designed to integrate with active safety systems, such as automatic emergency braking (AEB) and driver-fatigue detection systems. This allows the seat to work in conjunction with these systems to better protect passengers in sudden braking or collision situations. In electric and autonomous vehicles, interiors are often different from those in traditional vehicles, requiring new standards for seats. In autonomous vehicles, passengers may assume different seating positions, including semi-reclining and seats must be able to provide an adequate level of protection regardless of the setting.

In recent years, changes in automotive seat safety standards have focused on improving occupant protection against spinal injuries, enhancing safety in side and frontal crashes, integrating with advanced safety systems, and adapting seats to new electric and autonomous vehicles. In contrast, less attention has been paid to offset rear crashes, particularly in the context of the dynamic loads acting on people riding in the rear seats of a

vehicle. Rear-end crashes occur when the primary impact force acts from the rear of the vehicle, leading to deformation of the body. This type of collision can be observed especially in urban traffic conditions, where frequent and sudden braking is required. In this type of collision, the primary human protective function is performed by the seat back, headrest, seat belt, and the energy-absorbing structure of the vehicle body, sometimes supplemented by an energy-absorbing bumper [5, 6]. Such accidents usually result in head and neck injuries, including Whiplash (whiplash-type injuries), leading to damage to neck muscles, tendons, intervertebral discs, and nerves of the neck region. It is also known that the dynamic loads of rear-seat riders are often several times greater than those of front-seat occupants, where protection systems are much less developed than for front-seat occupants [7].

An important issue in ensuring safety during rear-end collisions are headrests on car seats, which protect the head and upper spine during a collision. The protective effect of headrests results from an integral part of the seat backrest, which together protects against injuries to the upper spine [8], which is particularly effective in the case of various types of active headrests [9]. The lack of or incorrect adjustment of the headrest can lead to serious injuries, including concussion and separation of the cervical vertebrae. Standard headrests can be adjusted manually, but their correct adjustment is often underestimated, which significantly reduces their effectiveness. Studies have shown that the best protection is provided when the headrest is located at the height of the center of the head, and the distance from it is a maximum of 6 cm [10]. The work also states that in the case of rear-end collisions, after full contact of the torso with the seat backrest, the torso is accelerated, while the head remains in its initial position for a very short time of 15–20 ms. The significant head acceleration occurs after 60-90 ms. This delay in the head acceleration to the torso causes relative movement of these body parts. The role of the headrest should be to reduce the relative movement. In [11] was shown, that increasing the backrest angle can effectively reduce the risk of excessive neck extension, which leads to a fracture at the base of the skull. The studies described in [12] showed that seats rated as good by the IIHS (Insurance Institute for Highway Safety) differed from poor mainly at speeds above 6 km/h in terms of loads

and moments acting on the neck, which suggests the need for further research on injury prevention systems. In [13] was reported that the seat belt significantly affects the dynamic loads of the passenger sitting in the rear on the left side during an oblique frontal collision, effectively reducing the head acceleration and shear forces of the neck at collision angles from 10° to 20° , but increasing the head acceleration at angles between 35° and 40° . The results of studies on the protective function of seat belts in the case of rear collisions are ambiguous. Some results of experimental studies using dummies indicate that the three-point seat belt system does not have a significant effect on the dynamic loads of a human [14], but computational models have shown that the seat belt, by increasing the force pressing the person to the seat surface, causes an increase in the friction force between the passenger and the seat backrest, which reduces the movement of people inside the cabin, and thus the risk of hitting rigid elements of the vehicle interior. In general, it is of course confirmed that seat belts, together with an airbag reduce the risk of injuries [15, 16], and the sliding of a person under the belt is less important. In [17, 18] it is stated that wearing seat belts reduces the risk of serious injuries in the event of rear-end collisions. During rear-end collisions, the airbag is not activated, therefore it is important to position the human body correctly so that, for example, at low values of the coefficient of friction between the person and the seat and at a greater backrest inclination, the person does not slide out from under the belts. According to [19], work is necessary to focus on introducing construction materials that absorb impact energy in the seat backrests, reducing contact with the side interior and the B-pillar. In [20] it is stated that at low speeds of rear-end collisions, the use of seat belts does not affect the dynamic loads of the head in a significant way. The studies described in [16] have shown that the position of the seat belt has a greater effect on chest deflection and rib stress than the belt angle, which indicates the need to optimize the restraint system to increase the protection of the passengers' chest during frontal collisions. The research described in [21] indicates that the introduction of an arc-shaped bumper beam increases energy absorption almost threefold, which significantly affects the value of dynamic head loads.

The qualitative assessment of the protective function of safety systems is therefore difficult

and should be considered individually, because it depends on many factors, including vehicle design, e.g. body shape, backrest tilt of the rear seats, headrest position, as well as individual human parameters, e.g. height, weight, muscle structure, especially for older people, which is manifested by a decrease in the values of damping parameters and stiffness of the musculoskeletal system [22]. Statistical quantitative assessment is practically impossible. The results of experimental studies presented in the literature in the analyzed case cannot be generalized due to the uniqueness of the motion conditions, e.g. position and type of obstacle, initial vehicle speed, etc. The protective function of various systems, e.g., headrests and seat belts in rear collisions, can be assessed using computer simulation [23]. Various biodynamic models can be found in the literature since the beginning of the 20th century. Biodynamic models can be divided into three main categories, consisting of bodies: rigid connected by elastic-damping elements, deformable, and using the finite element method (FEM). Many tools support the construction of original computational models enabling the introduction of motion equations, e.g. Excel or Matlab/Simulink, Fortran, and those that contain ready-made computational models using rigid body dynamics (e.g. PC-Crash, MSC.ADAMS, SIMPACK environment) or FEM, which is possible in environments such as Madymo, LS-Dyna. In construction practice, research using FEM dominates, while in the practice of research on road accidents and their effects in quantitative and qualitative terms, it is convenient to use the modeling of the dynamics of the motion of rigid bodies (vehicles or human), which was used, for example, in [24-27]. Simulation studies conducted using commercially available tools, e.g. PC-Crash, allow for the use of high numerical efficiency, leading to the possibility of examining a wide field of the influence of important parameters on the development of dynamic loads on humans in a short time [28]. The main advantage results from the possibility of using them together in one program: rigid body dynamics models describing vehicle movement, collision models, and multi-body systems describing human movement, using global and local coordinate systems, enabling a transformation of one system to another [32].

Research on dynamic loads on the human head during a road accident, especially in the context of a rear-end collision with a rigid obstacle, is

an area of significant importance in vehicle safety and injury prevention. However, several key research gaps result from:

- limitations of existing biomechanical models;
- shortage of data on design and operational parameters regarding the integrated safety system in the mutual coincidence of the headrest, backrest, seat, seat belt, and energy-absorbing structure of the vehicle body;
- diversity of cases in real road accidents.

Most previous studies have used biomechanical models and mannequins (e.g., Hybrid III) to simulate crashes and assess dynamic head loads. These models do not always faithfully represent the complex biomechanics of the human body, especially in the cervical-cranial system. Rear impacts induce complex interactions between the cervical vertebrae and the skull, and current models may not fully capture these nuances. A research gap exists in the area of more accurate biomechanical modeling of the human head and neck in real road accidents. Studies on dynamic head loads during crashes focus on studies, particularly in frontal and side impacts. However, there is a lack of data on the protective effectiveness of all passive safety elements in rear impacts, i.e. rear structure, seat, seat adjustment, backrest, headrest, and safety bassinet. The research gap, therefore concerns the need for multi-variant approaches, especially in the context of searching for the best configurations of design parameters, i.e., headrest stiffness, and operational parameters, i.e., setting the headrest, seat, and backrest angles to minimize the risk of head injury. Most studies are conducted on standard impact simulations, which assume certain idealized conditions, such as obstacle stiffness or ideal road conditions. Real accidents differ in terms of impact angle, type of obstacle, speed, and passenger body position. The research gap exists in the need for more diverse studies, taking into account the variety of accident scenarios, which could lead to more realistic conclusions and recommendations regarding head and neck protection. The above indicates that although there are many studies on dynamic head loads during rear impacts against a rigid obstacle, there are still some research gaps. These include both imperfections in biomechanical models and the lack of sufficient research on the influence of design and operational parameters of the seat with an integrated safety system. The article constitutes a significant extension of

knowledge concerning the influence of design and operational parameters of the seat, together with the integrated safety system on the generation of dynamic loads of the human head during a road accident. The challenge was taken up concerning solving key problems – research gaps in the scope of:

- the process of reconstructing similar accidents in the scope of proposed models, adopted input data for modelling;
- for designers during design or selection of headrests in the scope of their stiffness;
- for operators during vehicle operation in the scope of the angles of headrests, seat backrests, and seat adjustment.

DESCRIPTION OF THE CONSTRUCTED MODEL OF THE DYNAMICS OF THE COLLISION PROCESS

Description of the calculation tool used

The vehicle motion model was constructed in the PC-Crash 10.0 environment, using simulation modules covering vehicle dynamics, crash mechanics, and multi-body systems representing passengers. The built-in dynamics models allowed obtaining reliable results. The adopted integration step is 15 ms, which ensures sufficient simulation accuracy.

Description of vehicle dynamics models and rear-seat passengers

The spatial model of vehicle dynamics is characterized by six degrees of freedom, which allows for a detailed representation of vehicle motion in real conditions. Initial modeling conditions are as follows:

- a linear tire model was used for the cooperation of the tire with the roadway;
- the vehicle moved at an initial speed of $V_p = 80$ km/h.

A single-body model of vehicle motion dynamics, an energy-absorbing barrier model, and multi-body passenger models were used. The vehicle was loaded with the mass of people traveling: the driver and passengers. The applied models of vehicle motion dynamics, people, and collision were positively verified in [29, 30], which confirms their reliability in the context of research

on the dynamics of dynamic loads acting on the human body. The motion of each component of the multi-body system (the multi-body human model) is described by Newton's and Euler's equations [28]:

$$m_i \ddot{r}_i = \sum_{j=1}^l F_j \quad (1)$$

$$T_i \dot{\omega}_i + \omega_i \times T_i \omega_i = \sum_{j=1}^l M_j \quad (2)$$

where: i – element number of the multibody system;

j – external force number;

l – number of external forces acting on the component of the polyhedral system;

m_i – mass of the component of the polyhedral system;

\ddot{r}_i – acceleration of the centre of mass in the global system;

F_j – the external force acting on the component, expressed in the global system;

M_j – moment of external forces acting on the element, expressed in the local system;

T_i – tensor of inertia in the local system;

ω_i – angular velocity in the local system;

$\dot{\omega}_i$ – angular acceleration in the local system.

The load on the j th component of a multi-body system, e.g., the head, results from both: the force of gravity and contact forces, as well as other components of the multi-body system, e.g., the neck and torso, which act on the head through joints. When deriving the equations of motion of a multi-body system, one should not ignore the deviation moments in the inertia tensor, which in the case of vehicles, can be done with a fairly good approximation. Therefore, equations 1–2 can be simplified to the following form (ignoring the deviation moments in the inertia tensor):

$$m\ddot{x} = \sum_{j=1}^n F_{xj} \quad (3)$$

$$m\ddot{y} = \sum_{j=1}^n F_{yj} \quad (4)$$

$$m\ddot{z} = \sum_{j=1}^n F_{zj} \quad (5)$$

$$I_x \dot{\omega}_x + I_z \omega_y \omega_z - I_y \omega_y \omega_z = \sum_{j=1}^m M_{xj} \quad (6)$$

$$I_y \dot{\omega}_y + I_z \omega_x \omega_z - I_x \omega_x \omega_z = \sum_{j=1}^m M_{yj} \quad (7)$$

$$I_z \dot{\omega}_z + I_y \omega_x \omega_y - I_x \omega_x \omega_y = \sum_{j=1}^m M_{zj} \quad (8)$$

where: m – mass of the car;

x, y, z – coordinates of the beginning of the inertial coordinate system of the car's center of mass in the global system;

I_x, I_y, I_z – moments of inertia of the car body relative to the center of mass, expressed in the local system;

$F_x, F_y, F_z, M_x, M_y, M_z$ – external forces and moments, respectively, acting on the car, forces in the global system, moments in the local system;

$\omega_x, \omega_y, \omega_z$ – projections of the angular velocity vector of the car in the local system.

The following car parameters were assumed: length 4.2 m, width 1.7 m, height 1.4 m, distance of the center of mass from the front axle – 1.31 m, from the ground – 0.5 m, the moments of inertia are as follows: $I_x = 450 \text{ kg}\cdot\text{m}^2$, $I_y = 1498 \text{ kg}\cdot\text{m}^2$, $I_z = 1498 \text{ kg}\cdot\text{m}^2$; wheelbase 2.62 m, stiffness coefficient of the front and rear suspension (left and right side separately) 17576 N/m, 1977 N/m, front and rear stabilizer stiffness (separately) 8788 N/m. The basis for the selection of the values adopted is the PC-Crash program library. Passengers sitting in the rear seat were modeled using multi-body systems with multiple degrees of freedom, namely:

- two 50th percentile human models represented by 20 hyper-ellipsoid-shaped rigid solids (each) that were linked in kinematic chains using 19 spherical joints, the coefficient of friction between the solids and the seat is $\mu = 0,6$, which is consistent with the results presented in [31];
- two models of front seats and one model of rear bench seats represented by 13 rigid lumps (each) of hyper-ellipsoid shape, which were connected in kinematic chains using hinges.

The seat belts consist of two parts: chest and hip with a stiffness of 10,000 N/m and damping of 1000 N·s/m. The maximum force transmitted by the seat belts is 1 GN (1 giga Newton), and the pre-tension of the seat belt is 0 N.

Energy-absorbing barrier model and collision model

The barrier consists of 11 interconnected elements with the following parameters:

- dimensions and mass of each element: length 1.9 m, width 0.46 m, height 0.87 m, the center of mass of each element is at the geometrical center of the element, the moments of inertia are as follows: $I_x = 62 \text{ kg}\cdot\text{m}^2$, $I_y = 559 \text{ kg}\cdot\text{m}^2$, $I_z = 559 \text{ kg}\cdot\text{m}^2$; rotational resistance at the point of

contact concerning the axes: horizontal longitudinal (direction in line with the longer edge of the barrier) $S_x = 1000 \text{ Nm}^\circ$; vertical $S_z = 3000 \text{ Nm}^\circ$, horizontal transverse (direction in line with the shorter edge of the barrier) $S_y = 0 \text{ Nm}^\circ$; stiffness of each element is $355,331 \text{ N/m}$;

- coefficient of friction between colliding objects $\mu = 0.5$, coefficient of restitution $k = 0.1$.

The barrier elements are spaced 0,05 m apart and are connected in a chain. The above-mentioned values are proposed in the PC-Crash program and presented in [28]. The barrier is a kinematic chain of connected solids, moving as a result of impact forces. The movement of the above-described chain is influenced by forces generated in the connections between the elements. More details on the construction of the energy-absorbing barrier are described in [28]. The barrier elements are attached and can be rotated. Due to the lack of possibility to include in the program supports fixed in the ground, including their bending and tilting in the ground, the set of barrier elements will be most similar to an energy-absorbing barrier attached at the edge of the roadway. The resistance of the bent and displaced post in the ground at the stage of the impact of the front right wheel will be replaced by the friction of the blocks, while the post supporting the barrier will be replaced by a cylinder of relatively high mass and stiffness ($m = 500,000 \text{ kg}$, $I_z = 15,862 \text{ kg}\cdot\text{m}^2$, $S = 98,100,000 \text{ N/m}$). A rigid model was used to model the collision process, in which the velocities and accelerations of the bodies are calculated as a function of time. When a collision is detected, the vehicle is represented by several hyperellipsoids, consisting of 8 solids, 4 of which represent a solid and the other 4 represent wheels. The forces occurring in the contact

areas between the vehicle and the energy-absorbing barrier were represented using the coefficient of friction between the colliding objects. This coefficient, as a substitute parameter, is selected taking into account: metal-on-metal friction, interlocking of the bent sheet metal of the vehicle and the barrier, and tearing of the sheet metal of the right side door of the vehicle, and is $\mu = 0.5$, the coefficient of restitution $k = 0.1$. The view of the prepared model of the vehicle collision process with an energy-absorbing barrier is shown in Figure 1 and 2.

In the next step, calculations were performed to obtain the course of the process of the car hitting the energy-absorbing barrier. A silhouette view of the car during the analyzed event at selected moments is shown in Figure 3.

Preliminary (exploratory) calculations were carried out to determine the initial distance of the vehicle from the barrier. To obtain the rear-end rotation described in item 2 above, under the analyzed road conditions, on a wet road surface, with the assumed tire-road adhesion coefficient $\mu = 0.5$, an initial angular velocity relative to the vertical axis (VkZ) was introduced in the simulation. Reconnaissance calculations show that the vehicle, for the assumed initial distance from the barrier, will obtain the angle of rotation described above in p. 2 for an angular velocity of $VkZ = -3,5 \text{ rad/s}$. The results of these calculations indicate a satisfactory correspondence of the simulated movement of the vehicle in this stage of movement with the course of the accident. If a different value of speed VkZ is assumed, the distance of the vehicle from the barrier would be different, and at the moment of contact of the right side with the energy barrier, the speed is $VkZ = 0 \text{ rad/s}$. Therefore, the aspect of the influence of speed VkZ and the initial distance will not be considered further.

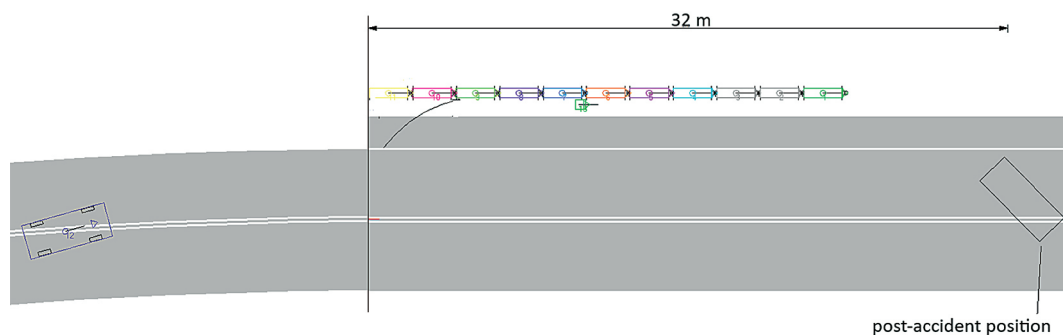


Figure 1. View of the prepared model of the process of vehicle collision with an energy barrier (top view)

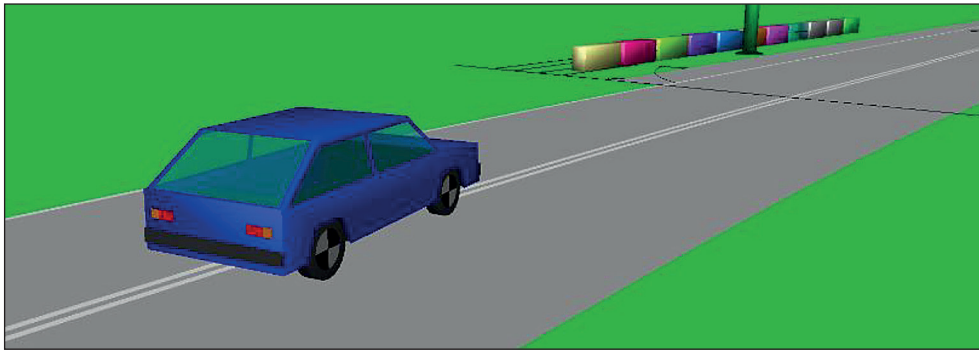


Figure 2. View of the prepared model of the impact with the energy barrier at the start of the simulation, $t = 0$ s (isometric view)

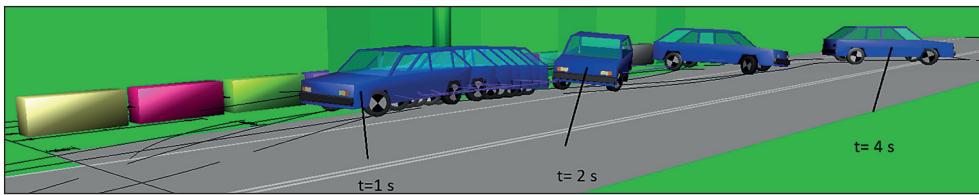


Figure 2. View of the prepared model of the impact with the energy barrier at the start of the simulation, $t = 0$ s (isometric view)

The obtained results of calculations presenting the silhouettes of the car, directions and returns of displacement vectors during the analyzed impact, areas of car contact with the barrier, and the post-accident position of the car are consistent with the revealed traces (car and barrier damage) and the course of the road event resulting from the analysis of evidence. The model of the car's movement was therefore considered reliable and proceeded to be used in further calculations of the dynamic loads acting on a person. In this stage of the work, the time was determined at which the first contact of the car with the barrier occurred ($t = 0.9$ s) and the last contact of the car with the barrier ($t = 2.7$ s).

The loads acting on the passenger seated on the rear seat on the left side during the impact of the car with the barrier were determined. Given the above, calculations of the dynamic loads on the seat occupant will be carried out at $t = 0.9$ – 2.7 s, where $t = 0$ s is the start time of the car. A multi-body model of the human seated on the rear seat on the right side was also considered, as it may affect the movement and dynamic loads of the passenger seated on the rear seat on the left side. The lumped parameters of the passenger models provided in the calculation program package were adopted. A view of the car model with rear-seat passengers is shown in Figure 4.

CALCULATION OF THE DYNAMIC LOADS ACTING ON THE LEFT REAR SEAT PASSENGER, SITTING FURTHER AWAY FROM THE OBSTACLE

Description of the adopted configurations

Having the models prepared: the dynamics of the car movement, the impact, the energy absorbing barrier, the passengers on the seats, and multivariant simulations of the traffic event were carried out, which took into account:

- headrests with different stiffness versions: $A0 = 20,000$ N/m, $A1 = 15,000$ N/m, $A2 = 10,000$ N/m, $A3 = 5000$ N/m, for a single value of the restitution coefficient $k = 0.1$;
- headrest tilt angle from vertical axles (Alfa 1 = 0° , Alfa 2 = 5° , Alfa 3 = 10° , Alfa 4 = 15°);
- backrest tilt angle from horizontal axle: OP55 = 55° , OP65 = 65° , OP75 = 75° ;
- seat tilt angle: $s0 = 0^\circ$, $s5 = 5^\circ$, $s10 = 10^\circ$, $s15 = 15^\circ$.

The passenger's seating position is determined by the vehicle's interior design. The distance of the head from the headrest varies depending on the adopted configuration of the backrest and headrest angle setting. The adopted configurations of the headrest tilt angle and backrest tilt angle are shown in Figure 5.

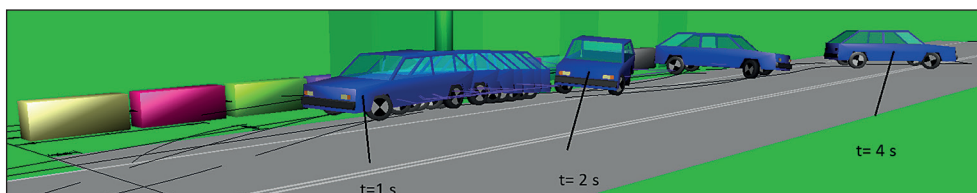


Figure 3. Silhouette view of the car during the analyzed incident at selected moments

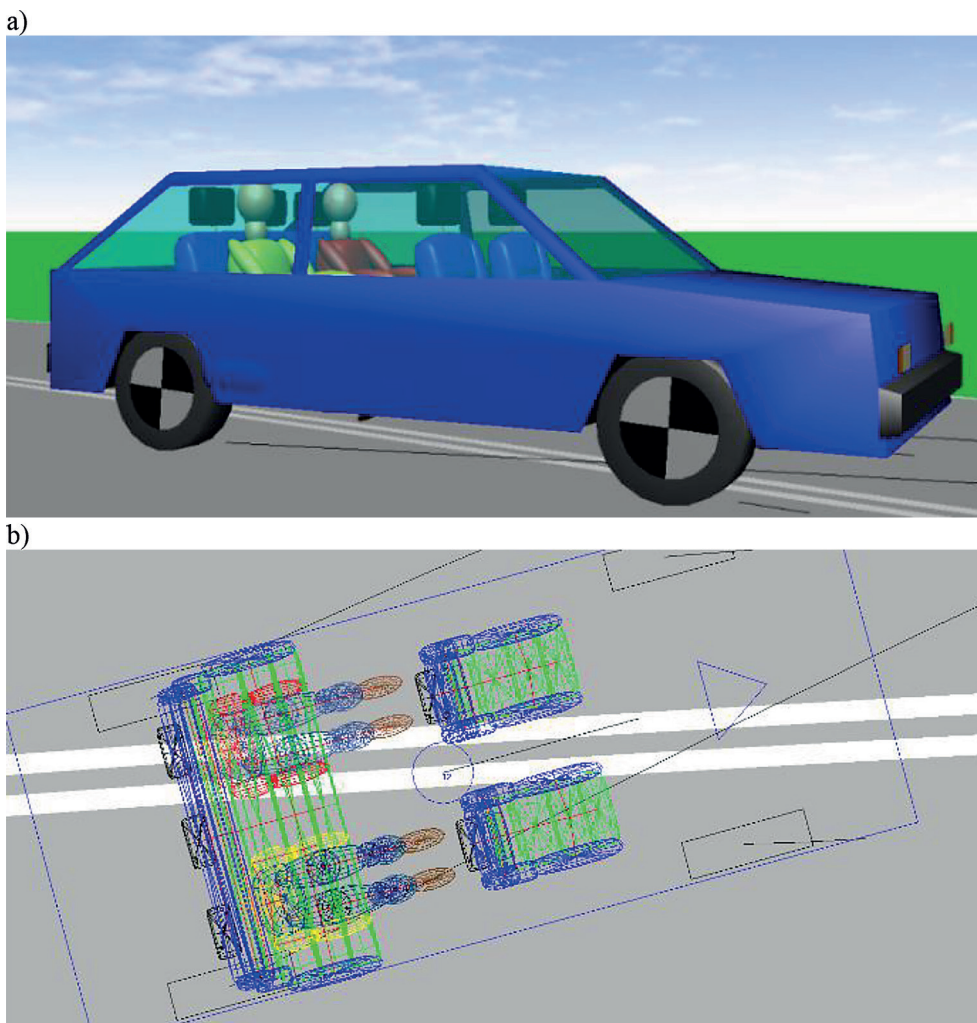


Figure 4. View of passenger models seated on the rear seat, a) isometric view, b) top view

The result of the calculations carried out is the waveforms of dynamic loads on the head (accelerations) of this passenger during a road accident. The reference systems in which the analyzed dynamic loads will be considered are local mutually perpendicular coordinate systems rigidly connected to the solids.

Of the 132 configurations considered and further presented, the results of the simulation calculations are sought to be the most favorable, to minimize the dynamic loads on the human

head during the traffic accident analyzed. Tables 1 and 2 show the results of the Head Injury Criterion (HIC_{36ms}) value calculations.

Analysis of the protective effectiveness of the headrest

The calculation results of the dynamic loads of the passenger depending on the considered variants at a backrest inclination angle of 55° (OP55), 65° (OP65), and 75° (OP75) are shown in Figures 6–8.

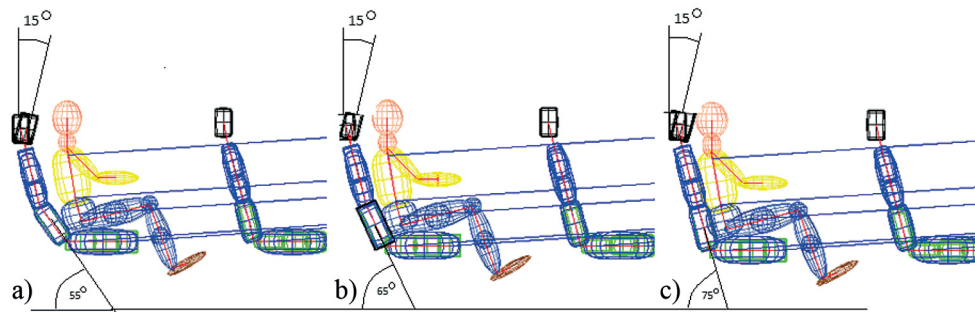


Figure 5. The adopted configurations of headrest tilt angle and backrest tilt angle (a) 55°, (b) 65°, (c) 75°

The analysis of the headrest’s protective effectiveness was carried out based on the determined values of the HIC_{36ms} coefficient, and the correlation coefficient of 1 was determined between the tables representing the increase in the OP angle value and the coefficient HIC_{36ms} .

There is a visible negative correlation of the HIC_{36ms} coefficient with the OP angle in each analyzed case. As the OP angle increases from OP55 to OP75, the HIC_{36ms} coefficient value decreases. This is primarily due to the decrease in the distance of the head from the headrest. In the case of stiffness $A0 = 20,000$ N/m, as the headrest angle increases, the HIC_{36ms} coefficient value decreases (negative correlation -0,595) for OP55, while as the headrest angle increases, the HIC_{36ms}

coefficient value increases (positive correlation 0,408 and 0,944) for OP65 and OP75. In the case of stiffness $A1 = 15,000$ N/m for the OP55 angle, the above values are strongly correlated (positive correlation 0.533); in the case of the OP65 angle, they are strongly negatively correlated (negative correlation -0.463), while in the case of OP75, they are weakly negatively correlated (negative correlation -0.073). In the case of stiffness $A2 = 10,000$ N/m, the above values are positively correlated for the analyzed angles OP55, 65, and 75 (respectively 0.907; 0.023; 0.462). In the case of stiffness $A3 = 5000$ N/m, the above values are positively correlated for OP55 and 75 (respectively 0.793 and 0.339), while for OP65 they are negatively correlated (-0.519).

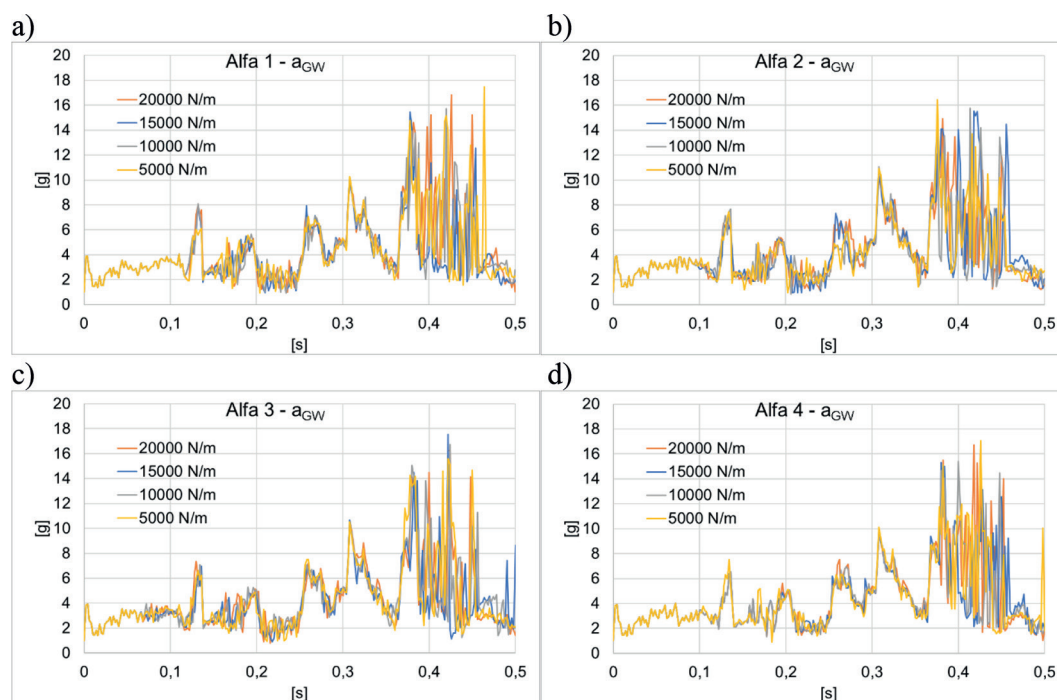


Figure 6. Results of calculations of dynamic loads of the passenger depending on the considered variants at a backrest inclination angle of 55°

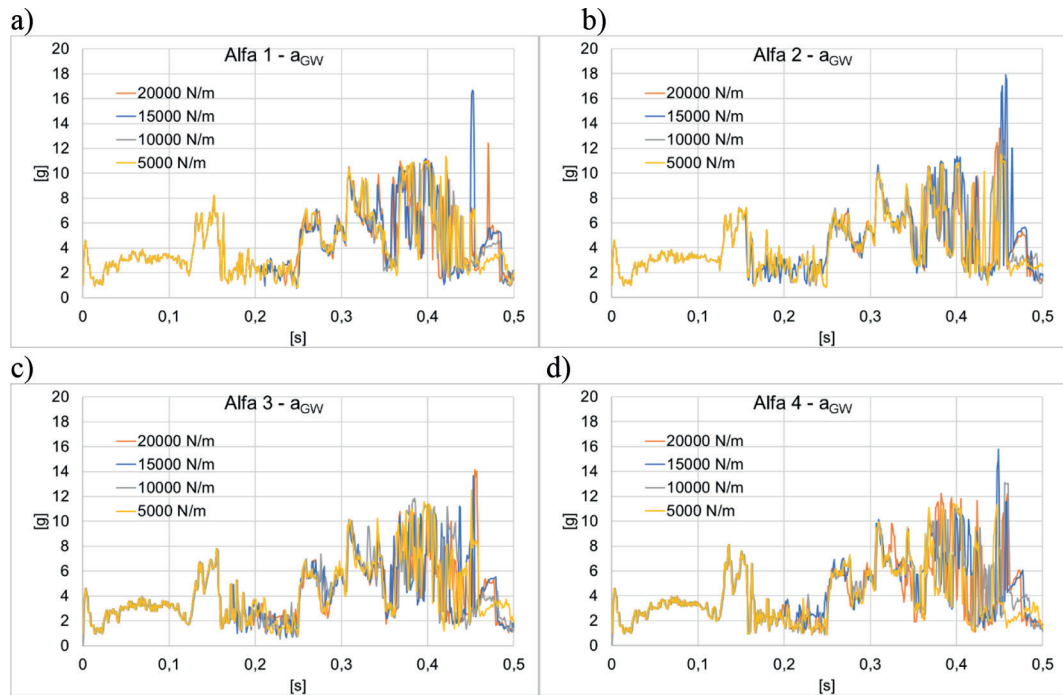


Figure 7. Results of calculations of dynamic loads of the passenger depending on the considered variants at a backrest inclination angle of 65°

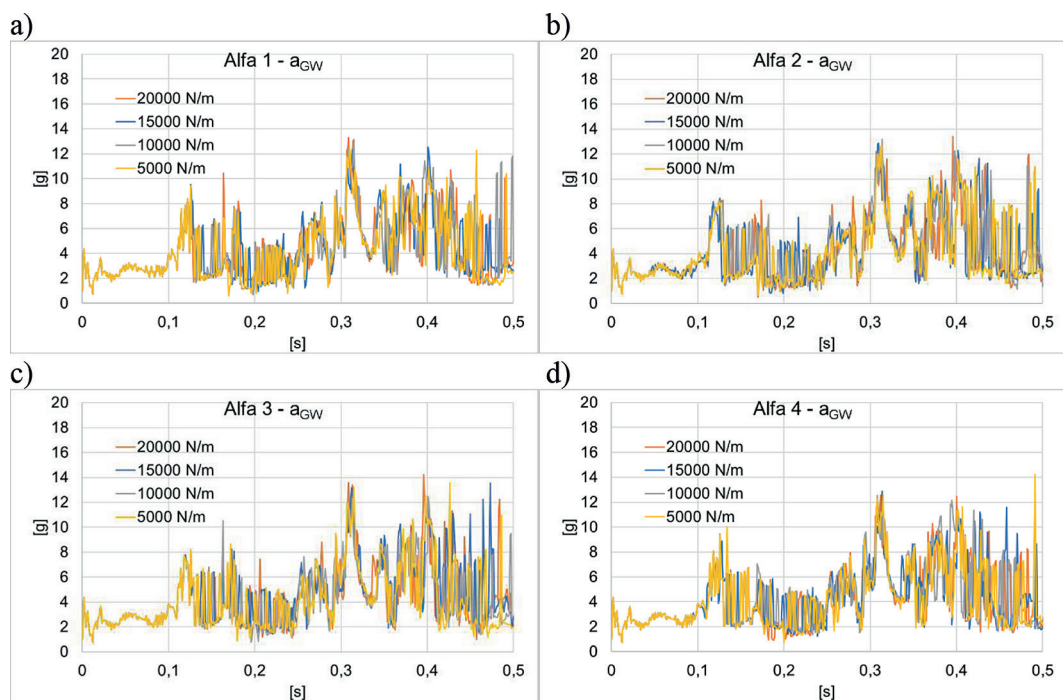


Figure 8. Results of calculations of dynamic loads of the passenger depending on the considered variants at a backrest inclination angle of 75°

Analysis of the protective effectiveness of the backrest and seat

The calculation results of the dynamic loads of the passenger depending on the considered

variants of the seat inclination at a backrest angle of 75°, 65°, and 55° are presented in Figures 9–11.

The analysis of the protective effectiveness of the backrest and seat was carried out based on the determined values of the HIC_{36ms} coefficient.

Table 1. Value calculation results in HIC_{36ms} – analysis of the protective effectiveness of the headrest

Parameters		HIC_{36ms}			Correlation coefficient 1
		OP55	OP65	OP75	
A0 = 20,000 N/m	Alfa 1=0°	10.0	7.0	6.1	-0.955
	Alfa 2=5°	9.9	6.0	6.2	-0.842
	Alfa 3=10°	7.7	6.3	6.3	-0.866
	Alfa 4=15°	9.1	7.7	6.3	-1.000
A1 = 15,000 N/m	Alfa 1=0°	5.9	6.7	5.8	-0.101
	Alfa 2=5°	8.1	7.1	6.1	-1.000
	Alfa 3=10°	5.9	5.4	5.3	-0.933
	Alfa 4=15°	8.6	6.4	6.0	-0.929
A2 = 10,000 N/m	Alfa 1=0°	6.7	8.0	6.5	-0.123
	Alfa 2=5°	6.6	5.8	6.4	-0.240
	Alfa 3=10°	9.5	9.7	6.1	-0.840
	Alfa 4=15°	9.8	6.8	7.1	-0.817
A3 = 5000 N/m	Alfa 1=0°	7.3	8.7	5.6	-0.548
	Alfa 2=5°	6.5	5.1	5.7	-0.569
	Alfa 3=10°	8.2	7.6	6.5	-0.986
	Alfa 4=15°	8.8	5.6	5.7	-0.852

The correlation coefficient 2 was determined between the tables, representing the decrease in the value of the stiffness coefficient of the seat and headrest and the HIC_{36ms} coefficient for selected seat inclination angles.

There is a strong correlation between the HIC_{36ms} coefficient and the OP angle in each analyzed

case. As the angle increases from OP55 to OP75, the HIC_{36ms} coefficient value decreases. This is primarily due to the increased distance of the head from the headrest. HIC_{36ms} values below 10 are considered low and pose no health risk. According to safety standards (FMVSS 208, Euro NCAP) and biomechanical tests, HIC_{36ms} values below 100

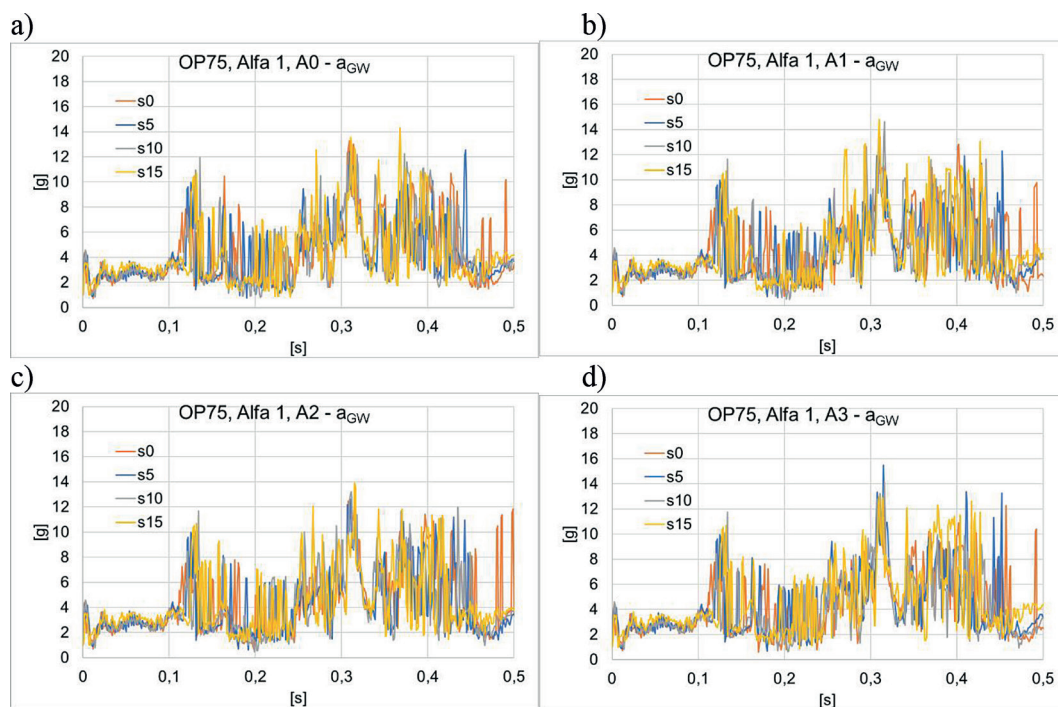


Figure 9. Results of calculations of dynamic loads of the passenger depending on the considered seat inclination variants at a backrest inclination angle of 75°

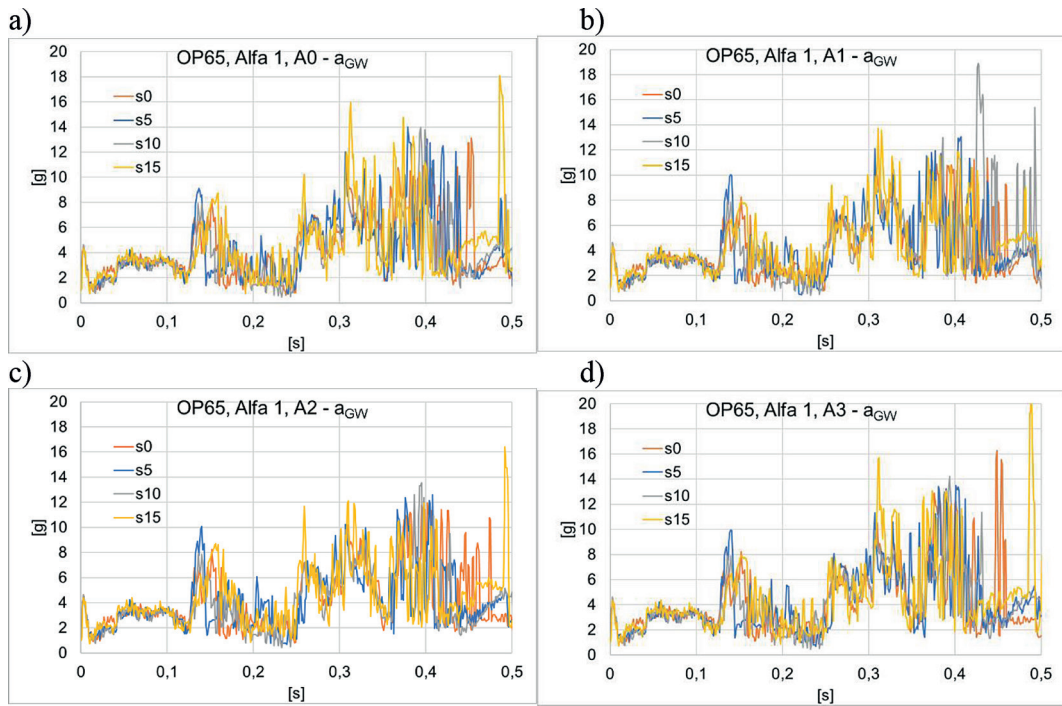


Figure 10. Results of calculations of dynamic loads of the passenger depending on the considered seat inclination variants at a backrest inclination angle of 65°

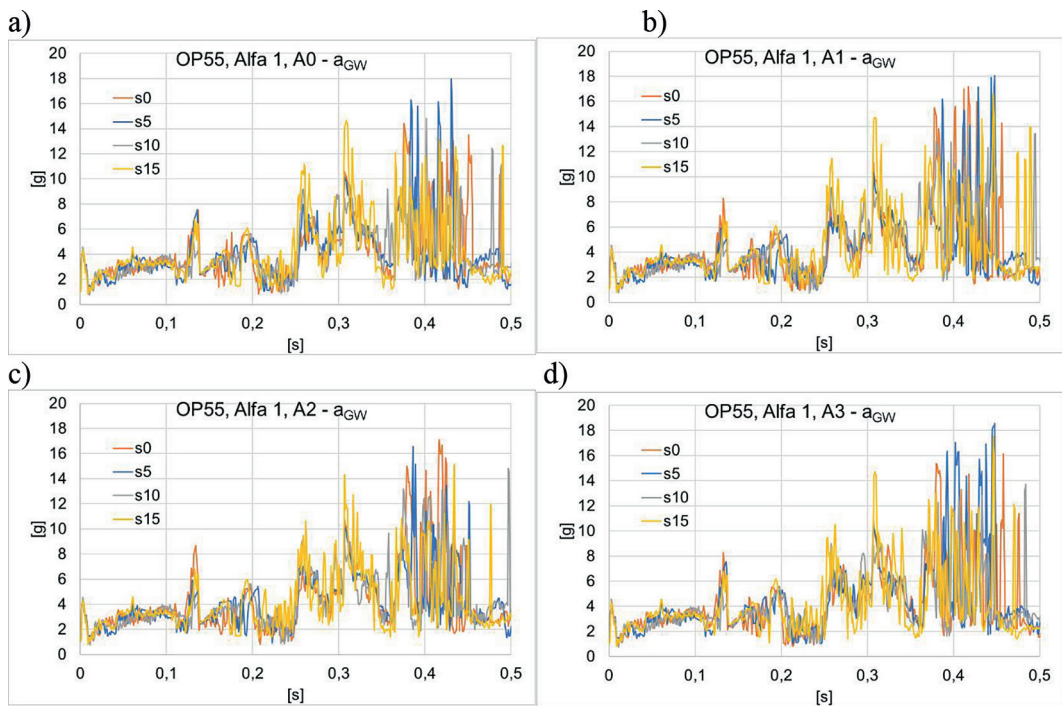


Figure 11. Results of calculations of dynamic loads of the passenger depending on the considered seat inclination variants at a backrest inclination angle of 55°

are considered safe and do not cause head injuries. The dynamic loads on the human head examined during the analyzed road accident allowed for the formulation of detailed conclusions:

- increasing the headrest inclination angle from Alfa1 to Alfa4 with a stiffness of $A0 = 20,000 \text{ N/m}$ causes a slight decrease in the HIC_{36ms} coefficient;

Table 2. Value calculation results in HIC_{36ms} – analysis of the protective effectiveness of the backrest and seat

Parameters		HIC_{36ms}				Correlation coefficient 2
		A0	A1	A2	A3	
s0	OP55	10	5.9	6.7	7.3	0.530
	OP65	7	6.7	8	8.7	-0.898
	OP75	6.1	5.8	6.5	5.6	0.264
s5	OP55	5.7	5.2	4.8	10.5	-0.680
	OP65	7.2	5.7	4.8	8	-0.134
	OP75	6.4	6.1	5.9	7.5	-0.561
s10	OP55	4.2	6.2	5.6	4.6	-0.085
	OP65	7.6	9.6	6.9	6.7	0.526
	OP75	7.2	7	7.2	7.7	-0.735
s15	OP55	7	5.7	6.1	5.9	0.653
	OP65	8.1	8.1	6.3	9	-0.103
	OP75	5.4	6.3	5.3	8.4	-0.718

- in variant 3, with the increase in the headrest inclination angle, the HIC_{36ms} values increase;
- the most unfavorable configuration is variant 1, in the Alfa1 configuration then the HIC_{36ms} values are the highest; – the most favorable configuration is variant 2 in the Alfa3 configuration, then the maximum HIC_{36ms} values are the lowest;
- for a headrest inclination angle of 5°, the HIC_{36ms} values decrease with the reduction of headrest stiffness;
- for variants 1 and 2, the lowest HIC_{36ms} coefficient values were achieved for the Alfa 3 configuration (10°), while for variants 3 and 4 for the Alfa2 configuration (5°).

ANALYSIS OF THE IMPACT OF HEADREST STIFFNESS AND INCLINATION ON HEAD INJURY RISK IN COLLISIONS

The analysis of the protective effectiveness of the headrest, backrest, and seat was carried out using the HIC_{36ms} coefficient, which measures the risk of head injuries in a collision. The influence of the OP angle (pitch deviation) and the stiffness of the headrest on this coefficient was examined. In general, a negative correlation was observed between the OP angle and the HIC_{36ms} value, i.e., the larger the tilt angle, the lower the HIC_{36ms} value, which means better protection. Higher stiffness ($A0 = 20,000$ N/m) caused a strong, negative HIC_{36ms} correlation for most angles, which indicates a lower risk of injury. At the lower stiffness ($A1 = 15,000$ N/m), the correlation was variable,

both positive and negative, depending on the OP angle. Stiffness A2 ($A2 = 10,000$ N/m) was characterized by weaker correlations, with a predominance of positive values for higher OP angles. In contrast, the stiffness A3 ($A3 = 5000$ N/m) showed similar trends, with correlations being mainly positive for OP55 and OP75, but negative for OP65. The conclusions indicate a significant effect of the headrest angle on the protective performance, especially at higher stiffnesses.

The HIC_{36ms} value decreased with increasing headrest angle from OP55 to OP75. The lowest HIC_{36ms} values were achieved for larger angles, suggesting better head protection with a more reclined backrest. However, the analysis showed differences depending on the seat angle, designated as s0, s5, s10, and s15. In some cases, the correlation was positive, while in others, it was negative, indicating the complexity of the effect of seat angle on protective performance. For example, for OP65 and s0, the correlation coefficient was negative (-0.898), indicating a strong inverse correlation. For OP65 and s10, the correlation was positive (0.526), which may indicate that a greater seat and backrest inclination angle may reduce protection. These results show that both the seat and backrest inclination have a significant impact on passenger safety. The correct configuration of angles is particularly important to minimize the risk of head injury.

The research provides new and important information on the impact of headrest geometry and stiffness on the risk of head injuries. These results have both scientific and practical significance, contributing to the design of safer car seats

and the optimization of existing solutions. New knowledge: These results show that head restraint stiffness is not linearly correlated with the risk of head injury, but its influence depends on the head restraint geometry (OP angle). It has been shown that smaller headrest angles may require less stiffness to provide low HIC_{36ms} values.

Directions for further research should be focused on the analysis of other types of vehicles, head mass, and impact velocity, including semi-reclining positions, leading to new standards for newly manufactured vehicles.

CONCLUSIONS

Conclusions from the analysis of the protective effectiveness of the headrest, backrest, and seat:

- the backrest angle (OP) has a significant impact on the level of head protection: the greater the angle of the OP (more reclined backrest), the lower the HIC_{36ms} – meaning a lower risk of head injury;
- the headrest with a high stiffness ($A0 = 20,000$ N/m) has strong negative correlation with HIC_{36ms} for most of its tilt angles;
- lower stiffnesses ($A1 = 15,000$ N/m – $A3 = 5000$ N/m) have variable correlations, dependent on OP angle – sometimes positive, sometimes negative; at lower OP angles, lower stiffness may be sufficient to achieve low HIC_{36ms} ;
- the impact of seat angle is complex – in some configurations, increasing the inclination improves protection; in others, it worsens it; for example: OP65 and s0 has strong negative correlation (-0.898) which means very good protection; OP65 and s10 has correlation also positive (0.526), which means reduce protection;
- it is no linear relationship between head restraint stiffness and head protection; the effectiveness of stiffness depends on the OP;
- the optimal configuration of backrest angle, seat angle, and head restraint stiffness can significantly reduce the risk of head injuries.

REFERENCES

1. Ptak M., Dymek M., Sawicki M., Fernandes F.A.O., Wnuk M., Wilhelm J., Ratajczak, M., Witkowska D., Kwiatkowski A., Poźniak B., Kubicki K., Tikhomirov M., Druszcz A., Chybowski L. Experimental and computational approach to human brain

modelling – aHEAD. Archives of Civil and Mechanical Engineering 2023, 10; 23(3): 218. <https://doi.org/10.1007/s43452-023-00758-9>

2. Ratajczak M., Ptak M., Chybowski L., Gawdzińska K., Będziński R. Material and structural modeling aspects of brain tissue deformation under dynamic loads. Materials 2019, 15; 12(2): 271. <https://doi.org/10.3390/ma12020271>
3. Ptak M., Fernandes F. A. O., Dymek M., Welter C., Brodziński K., Chybowski L. Analysis of electric scooter user kinematics after a crash against SUV. PLOS ONE 2022, 21; 17(1): e0262682. <https://doi.org/10.1371/journal.pone.0262682>
4. Jaśkiewicz M., Frej D., Matej J., Chaba R. Analysis of the head of a simulation crash test dummy with speed motion. Energies 2021; 8, 14(5): 1476. <https://doi.org/10.3390/en14051476>
5. Stańczyk T. L. Energochłonny zderzak tylny samochodu ciężarowego - element zapewnienia kompatybilności pojazdów. The Archives of Automotive Engineering. 2002; 22(1): 3–20.
6. Gidlewski M., Jackowski J., Posuniak P. Review and analysis of technical designs of rear underrun protective devices (RUPDs) in terms of regulatory compliance. Sensors 2022; 30: 22(7), 2645. <https://doi.org/10.3390/s22072645>
7. Żuchowski A., Wicher J. Wpływ wstępnego napięcia pasów bezpieczeństwa na obciążenia pasażerów na tylnych siedzeniach podczas zderzenia czołowego. The Archives of Automotive Engineering 2013; 61(3): 65–79.
8. Jaśkiewicz M. Analiza działania zagłówek mechanicznych z zerową prędkością wzdłużną względem głowy. Autobusy: Technika, Eksploatacja, Systemy Transportowe. 2011; 12(5): 175–80. <http://yadda.icm.edu.pl/baztech/element/bwmeta1.element.baztech-article-BWAN-0021-0024/c/Jaskiewicz.pdf>
9. Jaśkiewicz M., Stańczyk T. L. Ocena działania aktywnych zagłówek gazowych poprzez porównanie kinematyki ruchu zagłówek i manekina w próbie zderzeniowej. Teza Komisji Motoryzacji 2008; 33(34): 159–68.
10. Sokalski L., Waściszewski J. Koncepcja „aktywnego” zagłówka. Biuletyn WAT. 2006; 55(3).
11. Zhou H., Liao J., Zhang Q., Zhang G., Zhang D. Injuries analysis of rear row occupants exposed to vehicle’s frontal oblique collision. International Journal of Automotive Technology 2021; 31, 22(3): 595–607. <https://doi.org/10.1007/s12239-021-0056-9>
12. Mang D. W. H., Siegmund G. P., Blouin J. S. A comparison of anti-whiplash seats during low/moderate speed rear-end collisions. Traffic Injury Prevention 2020; 2, 21(3): 195–200. <https://doi.org/10.1080/15389588.2020.1718121>

13. Zhou H., Liao J., Zhang Q., Zhang G., Zhang D. Injuries analysis of rear row occupants exposed to vehicle's frontal oblique collision. *International Journal of Automotive Technology* 2021; 31, 22(3): 595–607. <https://doi.org/10.1007/s12239-021-0056-9>
14. Nilson G., Effects of Seat and Seat-Belt Design on Car Occupant Response in Frontal and Rear Impacts, A study combining mechanical and mathematical modelling, Department of Injury Prevention, Chalmers University of Technology S-412 96, Goteborg, Sweden.
15. Żuchowski A. Analysis of the influence of the vehicle impact velocity on the loads of the dummies in the front and rear seats. *The Archives of Automotive Engineering* 2018; 81(3): 159–76.
16. Edwards M. L., Parenteau C.S., Viano D. C. Front-seat occupant injuries in rear impacts: Analysis of the seatback incline variable in NASS-CDS. SAE Technical Paper 2009-01-1200, 2009. <https://doi.org/10.4271/2009-01-1200>
17. Parenteau C., Viano D.C. Field Data Analysis of Rear Occupant Injuries Part II: Children, Toddlers and Infants. SAE Technical Paper 2003-01-0154, 2003. <https://doi.org/10.4271/2003-01-0154>
18. Prasad P. An Overview of Major Occupant Simulation Models. SAE Technical Paper 840855, 1984. <https://doi.org/10.4271/840855>
19. Parenteau C., Viano D.C. Field Data Analysis of Rear Occupant Injuries Part I: Adults and Teenagers. SAE Technical Paper 2003-01-0153, 2003. <https://doi.org/10.4271/2003-01-0153>
20. Lawrence J.M., Siegmund G. P. Seat back and head restraint response during low-speed rear-end automobile collisions. *Accident Analysis & Prevention*. 2000; 32(2): 219–32. [https://doi.org/10.1016/S0001-4575\(99\)00108-6](https://doi.org/10.1016/S0001-4575(99)00108-6)
21. Hasegawa A., Fujii T., Matsuura N., Shimizu T. Load distribution structure of rear bumper beam to enhance vehicle body energy absorption in rear-end collisions. *Traffic Injury Prevention*. 2023; 21, 24(sup1): 75–9. <https://doi.org/10.1080/15389588.2023.2172573>
22. Jaśkiewicz M., Stańczyk T. L. The identification of damping and stiffness parameters of a driver model on the basis of crash tests. *Journal of KONES Powertrain and Transport* 2009; 16(1): 229–38.
23. Kim M.Y., Shin Y.S., Jeong J. Head behavior on left-turn across path and opposite direction crash using simulation. *Journal of Mechanical Science and Technology* 2023; 2, 37(5): 2537–2543. <https://doi.org/10.1007/s12206-023-0429-2>
24. Mnyazikwiye B.B., Karimi H.R., Robbersmyr K.G. Mathematical modeling of vehicle frontal crash by a double spring-massdamper model. In: *Communication and Automation Technologies (ICAT)*. Sarajevo; 2013.
25. Prochowski L., Gidlewski M., Ziubiński M., Dziewiecki K. Kinematics of the motorcar body side deformation process during front-to-side vehicle collision and the emergence of a hazard to car occupants. *Meccanica* 2021; 6, 56(4): 901–922. <https://doi.org/10.1007/s11012-020-01274-3>
26. Siminski P. Aspect of Simulation and Experimental Research Studies on Wheeled Armored Fighting Vehicles with Hydropneumatic Suspension. SAE Technical Paper 2010-01-0651, 2010. <https://doi.org/10.4271/2010-01-0651>
27. Działak P., Karliński J., Maślak P. Development of a biomechanical human model for safety analysis of the operators of self-propelled mining machines. *Acta Mechanica et Automatica*. 2024; 1, 18(2): 333–340. <https://doi.org/10.2478/ama-2024-0037>
28. Wach W. Symulacja wypadków drogowych w programie PC-Crash. Kraków: Wydawnictwo Instytutu Ekspertyz Sądowych; 2009.
29. Steffan H., Moser A. The Collision and Trajectory Models of PC-CRASH. SAE Technical Paper 960886, 1996.
30. Moser A., Steffan H., Kasanický G. The Pedestrian Model in PC-Crash - The Introduction of a Multi Body System and its Validation. SAE Technical Paper 1999-01-0445, 1999.
31. Jaśkiewicz M. Evaluation of the reliability of the shoulder and knee joint of the KPSIT C50 dummy adapted to crash tests carried out at low speeds. *Eksploatacja i Niezawodność – Maintenance and Reliability* 2024; 8, 26(1). <https://doi.org/10.17531/ein/178376>
32. Pusty, T., Mietań, M., Pilich, J., Simiński, P., Kupicz, W., Lewiński, R., Mysłowski, J., Research on the possibility of carrying out convoy driving missions using vehicles with varying degrees of autonomy. *Archives of Transport* 2024; 72(4): 7-21. <https://doi.org/10.61089/aot2024.xdtvm09>